Historical Biology
An International Journal of Paleobiology

ISSN: (Print) (Online) Journal homepage: https://www.tandfonline.com/loi/ghbi20

Early Miocene *Aprotodon* (Perissodactyla, Rhinocerotidae) from Northern China

Danhui Sun, Shijie Li, Shiqi Wang & Tao Deng

To cite this article: Danhui Sun, Shijie Li, Shiqi Wang & Tao Deng (01 Dec 2023): Early Miocene *Aprotodon* (Perissodactyla, Rhinocerotidae) from Northern China, Historical Biology, DOI: 10.1080/08912963.2023.2288618

To link to this article: https://doi.org/10.1080/08912963.2023.2288618

HISTORICAL BIOLOGY
https://doi.org/10.1080/08912963.2023.2288618

Taylor & Francis
Taylor & Francis Group

Early Miocene *Aprotodon* (Perissodactyla, Rhinocerotidae) from Northern China

Danhui Sun[a,b], Shijie Li[a,b], Shiqi Wang[b] and Tao Deng[a,b]

[a]University of Chinese Academy of Sciences, Beijing, China; [b]Key Laboratory of Vertebrate Evolution and Human Origins, Institute of Vertebrate Paleontology and Paleoanthropology, Chinese Academy of Sciences, Beijing, China

ABSTRACT

The genus *Aprotodon* is a special group of rhinoceroses, which has a very long survival time frame but a relatively limited distribution in Asia. Herein, we report on a well-preserved and complete skull found in the lower layers of the Zhang'enbao Formation from the Early Miocene age in Tongxin County, China. The morphology of the new specimen is different from all the known species of *Aprotodon* in its smaller size, with both sides of the parietal crest fused and forming a sagittal crest, the V-shaped anterior edge of the posterior nares positioned at the level of M2, the weak supraorbital tuberosity, the developed and multiple crista on premolars, and the reduced lingual cingulum, forming a pillar around the entrance of the medisinus on molars. Based on these, we refer the Tongxin specimen to a new species, *A. qiui* sp. nov. Phylogenetic analysis reveals that *A. qiui* sp. nov. and other members of *Aprotodon* are in a stable monophyletic clade. *A. qiui* sp. nov. is the sister taxon to *A. lanzhouensis*.

ARTICLE HISTORY
Received 23 October 2023
Accepted 23 November 2023

KEYWORDS
Aprotodon; osteology; phylogeny; Early Miocene; Northern China

Introduction

Aprotodon is a comparatively primitive and specialised taxon, currently found in Asia, including Pakistan (Pilgrim 1912; Forster-Cooper 1915), Kazakhstan (Beliajeva 1954; Borissiak 1954; Heissig 1972), and Gansu Province and Inner Mongolia in Northwest China (Qiu and Xie 1997; Qiu et al. 2004; Wang et al. 2009; Deng 2013; Li et al. 2021). The genus *Aprotodon* has a very long survival time frame. The earliest member of the genus *Aprotodon* was discovered in the Late Eocene Houldjin Formation near Erenhot, Inner Mongolia (Wang et al. 2009). Besides, Qiu et al. (2004) reported a skull and mandible of *Aprotodon lanzhouensis* found in the Late Oligocene deposits of the Linxia Basin, Gansu. Qiu and Xie (1997) reported a skull and several mandibles from the Early Miocene of the Lanzhou Basin, Gansu. In addition, Deng (2013) and Li et al. (2021) reported the latest member of the genus *Aprotodon* from the Early Miocene of northwestern China.

The genus *Aprotodon* was established by Forster-Cooper (1915) based on two mandibular symphyses from the Bugti Formation, Pakistan. Until now, the genus *Aprotodon* includes four species *Aprotodon smith-woodwardi* (Forster-Cooper 1915), *Aprotodon fatehjangensis* (Pilgrim 1912), *Aprotodon aralensis* (Borissiak 1954), and *Aprotodon lanzhouensis* (Qiu and Xie 1997). The fossils of the genus *Aprotodon* are scarce. For instance, *A. smith-woodwardi* only contains some mandible materials. *A. fatehjangensis* only has dental materials, including P4 and M2. *A. aralensis* contains a skull and a mandible. At present, *A. lanzhouensis* is the species with the most material in the genus *Aprotodon*.

Herein, we report on a well-preserved and complete skull found in the lower layers of the Zhang'enbao Formation from the Early Miocene age in Tongxin County, Ningxia Hui Autonomous Region, China. The morphology of the new specimen is different from all the known species of *Aprotodon*, leading to the description of a new species.

The fossils for this study are stored in the collection of the Institute of Vertebrate Paleontology and Paleoanthropology (IVPP), Chinese Academy of Sciences, Beijing, China. The fossils are described and identified through anatomical descriptions, comparative anatomy as well as biometrical measurements. Rhinocerotid terminology and taxonomy follow Heissig (1999), Guérin (1980), and Antoine (2002). Anatomical features described follow basically the same sequence as in Antoine (2002), and Antoine et al. (2010). The specimens were measured in accordance with the procedures described in Guérin (1980).

Systematic Paleontology

Order **Perissodactyla** Owen, 1848
Family **Rhinocerotidae** Gray, 1821
Tribe **Teleoceratini** Hay, 1902
Genus ***Aprotodon*** Forster-Cooper,1915

Type species

Aprotodon smith-woodwardi (Forster-Cooper 1915)

Other species

A. fatehjangensis (Pilgrim 1912), *A. aralensis* (Borissiak 1954), *A. lanzhouensis* (Qiu and Xie 1997)

Distribution

Late Eocene to Early Miocene, eastern and central Asia

Aprotodon qiui sp. nov.
(Figs 1–3; Tables 1–3)

Holotype

IVPP V 23533, a well-preserved and complete skull (Figures 1–2) representing an adult individual.

CONTACT Tao Deng dengtao@ivpp.ac.cn University of Chinese Academy of Sciences, Beijing 100049, China
Supplemental data for this article can be accessed online at https://doi.org/10.1080/08912963.2023.2288618

Published online 01 Dec 2023

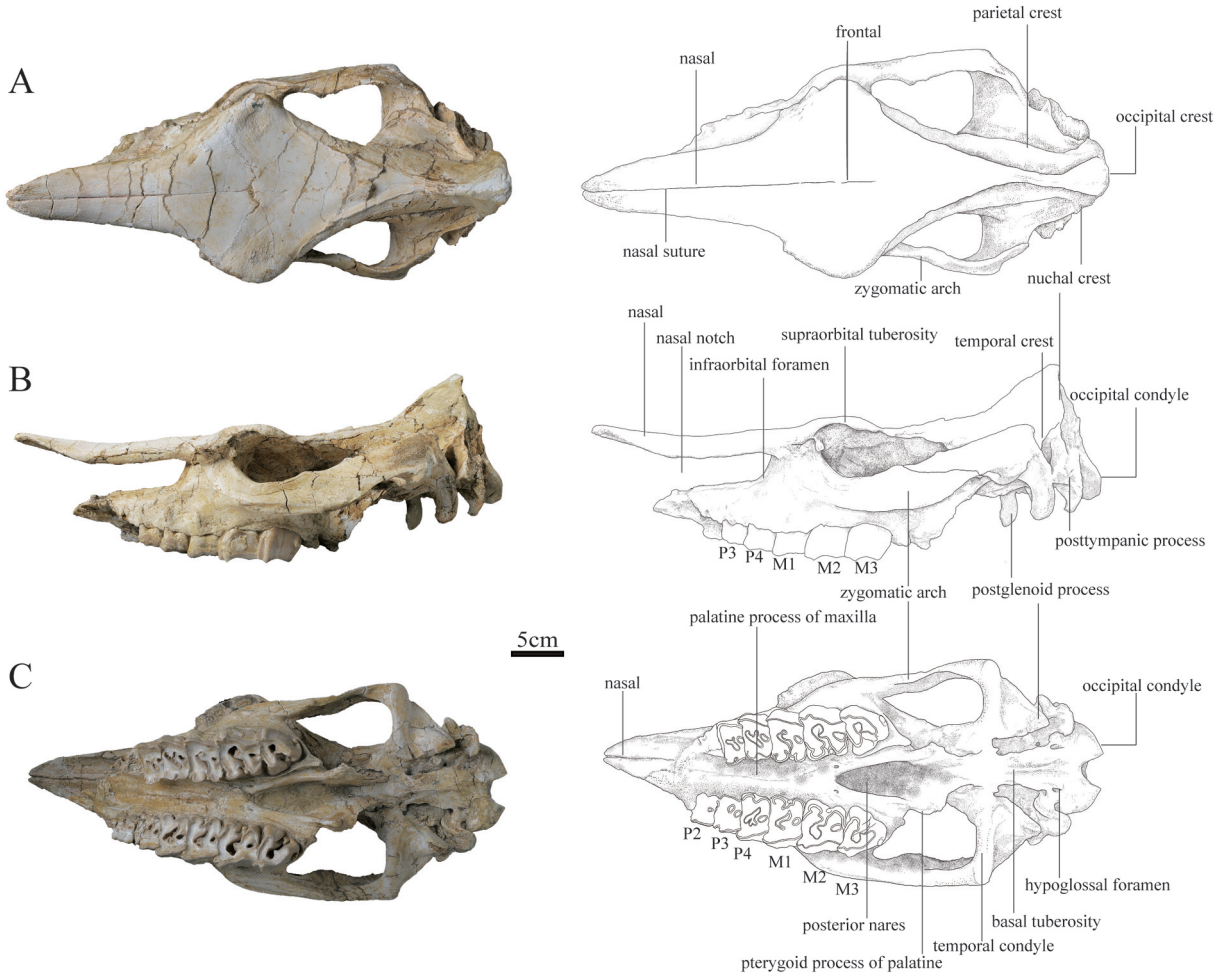

Figure 1. Photographs and sketches of the skull of *Aprotodon qiui* sp. nov., holotype (IVPP V 23533) A. dorsal view; B. lateral view; C. ventral view.

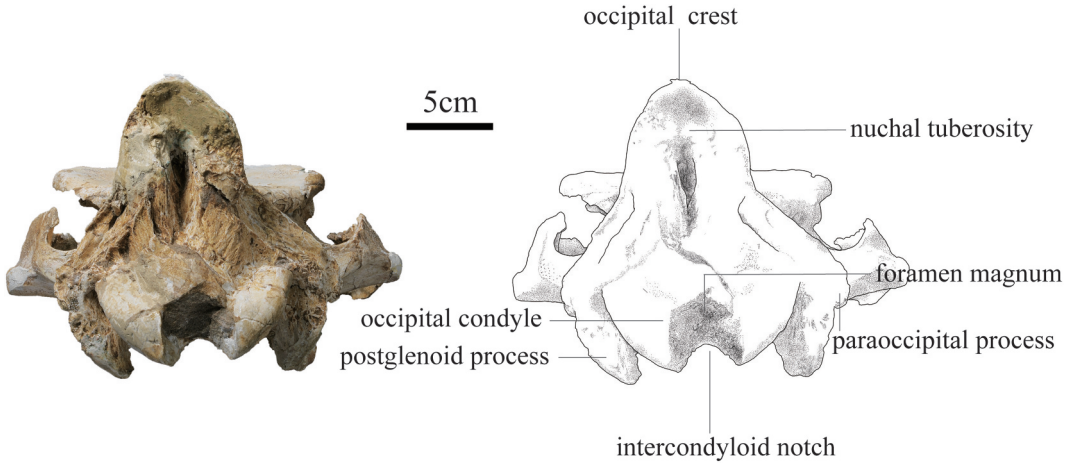

Figure 2. Photograph and sketch of the skull of *Aprotodon qiui* sp. nov., holotype (IVPP V 23533).

Derivation of name

The species name is in honour of Professor Zhanxiang Qiu, who has made great contributions to Neogene Paleontology and Stratigraphy in China.

Type locality and horizon

Miaoerling in Shishi Township, Tongxin County, Ningxia Hui Autonomous Region, China (NXTX201703A, N 37°00′39.13″, E 106°01′26.57″, H = 1452 m); Early Miocene.

Diagnosis

The skull is slender. The nasal bones are thin, long, and straight. The nasal notch is high and deep, with the posterior end at the level of the posterior part of P4. The anterior margin of the orbit is positioned at the level of the M2. The distance between the posterior edge of the nasal notch and the orbit is short. The parietal crest forms a sagittal crest. The anterior edge of the posterior nares is V-shaped positioned at the level of M2. The supraorbital tuberosity is developed. The crista is developed and multiple on premolars. The lingual cingulum is reduced on molars, forming a pillar around the entrance of the medisinus.

Differential diagnosis

Differs from *Aprotodon aralensis* in its smaller size, with both sides of the parietal crest fused and forming a sagittal crest, the V-shaped anterior edge of the posterior nares, weaker supraorbital tuberosity, and the reduced lingual cingulum on molars, forming a pillar around the entrance of the medisinus. Differs from *Aprotodon lanzhouensis* in having thinner nasal bones, posteriorly placed anterior margin of the orbit, strong crochet, developed and multiple crista on premolars, and the reduced lingual cingulum on molars, forming a pillar around the entrance of the medisinus. Differs from *Aprotodon fatehjangensis* in smaller size, weak crista on premolars, and the reduced lingual cingulum on molars, forming a pillar around the entrance of the medisinus.

Description

Skull

The skull of IVPP V 23533 is a well-preserved adult individual only lacking the premaxillary bone and left P2. The skull was slightly flattened by vertical compression, with the posterior part of the nasal bones collapsed downward and a little narrowing of the nasal notch.

In the lateral view, the skull is slender. The occipital part is suddenly raised, and its profile is almost anteriorly inclined with high and small occipital condyles. The posttympanic processes are short and fused with the paraoccipital processes, and anteriorly touches the postglenoid process. The pseudomeatus external auditory is closed ventrally with its short upper edge positioned in the lower half of the occipital crest. The area between the temporal and occipital crests is depressed. The zygomatic arch is thin whose anterior end is positioned at the level of M2 and close to the cheek teeth row, and the posterior end of the dorsal edge has a short process and rough surface. The temporal condyle articulated with the mandible is protruding from the ventral edge of the zygomatic arch. The postglenoid process is laterally flattened. The position of the dorsal margin of the orbit is high, and the anterior margin of the orbit is positioned at the level of the M2. The supraorbital tuberosity is developed. The postorbital process is present. The posterior orbital border is formed by the zygomatic bone. The nasal bone is particularly long and thin with lateral apophyses on both sides. The nasal notch has a U-shaped outline with its posterior edge positioned at the level of the posterior part of P4. The distance between the posterior edge of the nasal notch and the orbit is short, about 62.91 mm. The infraorbital foramen is located dorsally to the level of P4 and below the nasal notch.

In the dorsal view, the frontal surface of the skull is rhombic and flat, and the distance between the two sides of the parietal crest is very short, forming a single sagittal crest with its anterior part reaches the level of the posterior zygomatic arch. The sagittal crest is divided into two crests at its posterior end, forming a small triangular surface, and then backward, converging into the occipital crest. The zygomatic arch does not project strongly to the sides, and the widest part of the skull is located at the posterior end of the zygomatic arch. The ratio of zygomatic width to frontal width is less than 1.5. The widest position of the dorsal surface is located between the supraorbital processes, about 187 mm. The nasal bone becomes narrow gradually before the orbits (i.e. the nasal base does not have a constriction). The nasal bone is narrow, flat, and long with a nasal suture.

In the ventral view, the skull is long with a length more than 529 mm. The occipital and ventral surfaces of the occipital condyle are rounded. The hypoglossal foramen is laterally positioned, at the basement of the paraoccipital process. The posttympanic process is and fused with the paraoccipital process, and anteriorly touches the postglenoid process. The alar foramen is opened on the lateral wall of the posterior nares, anteroposteriorally at the level of the temporal condyle. The tympanic bulla was crushed, exposing the inner bones. The temporal condyle is high with straight transverse axis. The posterior margins of pterygoid are nearly vertical. The anterior edge of the posterior nares is V-shaped in outline, at the level of M2. The palate is quite wide laterally, narrowing in width as it extends forward. The buccal and lingual edges of the cheek teeth row are nearly straight.

In the posterior view, the occipital face is bell-shaped in outline, and the upper part is narrower than the lower part. The occipital crest is broken. The nuchal tuberosity is developed. The foramen magnum is small, rounded in shape, and its width is 38 mm. The occipital condyles are relatively small, and its lateral margin has a short and steep upper part, and a long and curved lower part. The width between exterior edges of occipital condyles is 97 mm.

Upper teeth

The upper teeth are moderately worn. The lingual edge of upper cheek teeth row is almost in a straight line posteriorly positioned relative to the orbit. On the upper cheek teeth, the constriction and expansion of the lingual cusps are developed; the buccal side of upper cheek teeth are covered by a spot of cement. On the premolars, the buccal wall is nearly straight; there is a lingual bridge between the protocone and hypocone; the protocone is constricted, and its lingual margin is curved; the crista is developed and multiple; the crochet is weak; the medisinus is closed; and the postfossette is narrow and closed. On the molars, both the crochet and antecrochet are developed and strong; the protocone and hypocone are strongly constricted; and the buccal cingulum is absent, and the lingual cingulum is reduced, forming a pillar around the entrance of the medisinus.

The left P2 is not preserved. The right P2 is fragmented, retaining the buccal portion. The right P2 is presumed to have smaller length than width on the basis of the residual structure. The parastyle fold and the paracone rib are developed. The postfossette is closed.

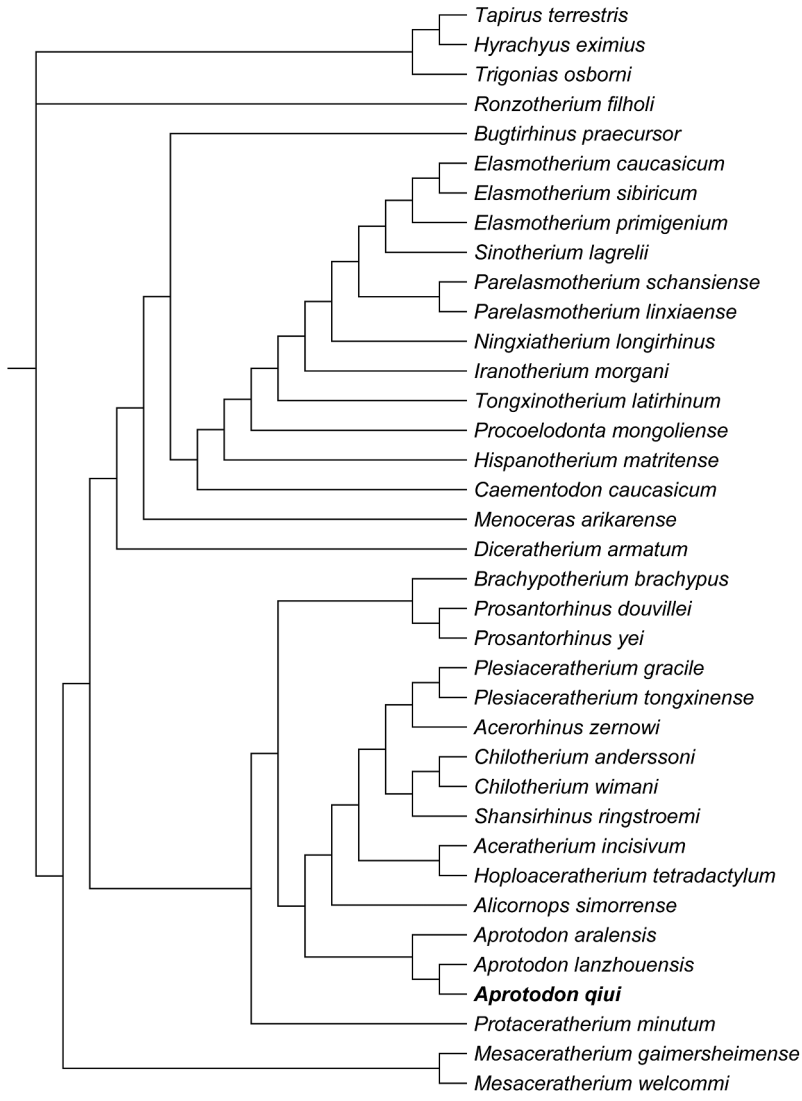

Figure 3. The most parsimonious tree, with 1225 steps in PAUP (consistency index = 0.2996; retention index = 0.5552), showing systematic position of *Aprotodon qiui* sp. nov.

Table 1. Measurements of the upper teeth of *Aprotodon qiui* sp. nov. compared with other *Aprotodon*. (mm).

Teeth		*A. qiui* sp. nov. IVPP V 23533	*A. lanzhouensis* (Qiu and Xie, Qiu and Xie 1997)	*A. aralensis* (Borissiak 1954)	*A. fatehjangensis* (Pilgrim 1912)
DP1	L	-	15.8	-	-
	W	-	16.8	-	-
	H	-	10.5	-	-
P2	L	21.57	24	26–27	-
	W	26.84	28	35–38	-
	H	9.98	17.5	-	-
P3	L	24.83	31.3	31–32	-
	W	40.81	43.7	42–48	-
	H	10.39	23.4	-	-
P4	L	30.42	35.2	36	44.5
	W	41.35	49.4	53–54	61
	H	15.62	26.2	-	-
M1	L	34.91	43	41–45	48
	W	47.95	50	58–59	60
	H	14.92	25	-	-
M2	L	42.45	51	50–52	63
	W	50.26	53	61–63	74
	H	22.38	37	-	-
M3	L	40.25	-	61–62	-
	W	47.34	-	55–58	-
	H	30.48	-	-	-

Table 2. Comparisons between *Aprotodon qiui* sp. nov. (IVPP V 23533) and other species of the genus *Aprotodon*.

Species/Characters	*A. qiui* sp. nov. IVPP V 23533	*A. lanzhouensis* IVPP V 13,852	*A. aralensis* (Borissiak 1954)	*A. fatehjangensis* (Pilgrim 1912)
paracone fold on the premolar	weak	strong	strong	strong
crista on the premolar	developed and stellate	absent	absent	-
lingual cingulum on the premolar	developed	developed	developed and continous	absent
crochet on the molar	strong	weak	absent	strong
antecrochet on the molar	strong	strong	strong	weak
lingual cingulum on the molar	reduced, forming a pillar	absent	-	absent
Distance between nasal notch and orbit	62.91 mm	50 mm	70 mm	-
Distance between nasal tip and bottom of nasal notch	164.21 mm	~180 mm	220 mm	-

Table 3. Measurements of the skull of *Aprotodon qiui* sp. nov. (IVPP V 23533). (mm).

numbers	measures	*Aprotodon qiui* sp. nov.
1	Distance between occipital condyle and premaxilla	~
2	Distance between occipital condyle and nasal tip	521.13
3	Distance between nasal tip and occipital crest	479.06
4	Distance between nasal tip and bottom of nasal notch	164.21
5	Minimal width of braincase	68.31
6	Distance between occipital crest and postorbital process	219.05
7	Distance between occipital crest and supraorbital process	251.12
8	Distance between occipital crest and lacrimal tubercle	287.16
9	Distance between nasal notch and orbit	62.91
13	Distance between occipital condyle and M3	236.13
14	Distance between nasal tip and orbit	234.11
15	Width of occipital crest	60.69
16	Width of paramastoid process	119.03
17	Minimal width between parietal crests	14.35
18	Width between postorbital processes	152.12
19	Width between supraorbital processes	187.06
20	Width between lacrimal tubercles	176.31
21	Maximal width between zygomatic arches	231.05
22	Width of nasal base	95.81
23	Height of occipital surface	114.21
25	Cranial height in front of P2	83.31
26	Cranial height in front of M1	86.63
27	Cranial height in front of M3	91.32
28	Width of palate in front of P2	37.86
29	Width of palate in front of M1	35.11
30	Width of palate in front of M3	52.04
31	Width of foramen magnum	34.55
32	Width between exterior edges of occipital condyle	92.53

P3 has a weak parastyle fold and paracone rib. The protocone is slightly larger than the hypocone. The crochet is weak. The medisinus is narrow and closed. The postfossette is closed and small in a round shape. The lingual cingulum is developed, and the buccal cingulum is absent.

P4 is similar to P3, but much larger. Both the protocone and hypocone are expanded, with constrictions. The hypocone is slightly smaller than the protocone. The lingual margin of the protocone is curved. The protoloph is a little bit longer than the metaloph. Both the medisinus and the postfossette are closed. The anterior cingulum is developed. The lingual cingulum is V-shaped at the entrance of the medisinus. The buccal cingulum is absent.

M1 has a nearly straight buccal wall. The strongly constricted protocone has a flat lingual margin, and the hypocone has a strong anterior constriction. The antecrochet is strong and elongates to the entrance of the medisinus. The medisinus is narrow and open. The postfossette is round in shape and closed. The buccal cingulum is absent.

M2 has a long parastyle and a developed parastyle fold, and a paracone rib. The protocone has developed anterior and posterior constrictions. The stout end of the antercrochet extends to the entrance of the medisinus. The antecrochet and hypocone are separated. M2 has an open medisinus, an oval-shaped and closed postfossette. The buccal cingulum is absent.

M3 has a quadrangular outline in occlusal view. It has a developed parastyle fold, and a paracone rib with an undulating buccal wall. The protoloph is transverse on the antero-lingual side. The protocone has slightly anterior and posterior constrictions. The posterior cingulum is reduced.

Comparison and discussion

The Tongxin specimen has typical features of hornless rhinoceros (Heissig 1989; Cerdeño 1995), including a flat and long nasal bone with a retracted nasal notch; the posttympanic process fused with the paraoccipital process; the constricted lingual cusps on the upper cheek teeth. However, the Tongxin specimen has suddenly raised occipital part and developed supraorbital tuberosity, unlike the genus *Plesiaceratherium* and *Acerorhinus* (Yan 1983; Qiu et al. 1988; Deng 2000). The

small size, thin, long, and straight nasal bones, slightly deeper nasal notch, and constriction of the protocone of the Tongxin specimen differs from the genus *Brachypotherium* (Geraads and Miller 2013). The Tongxin specimen has a small size, slender skull, developed supraorbital tuberosity, and developed and multiple crista on premolars, which are different from the genus *Alicornops* (Deng 2004). The premolars of the Tongxin specimen are semi-molarized with a lingual bridge between the protocone and hypocone different with those of the *Chilotheium* which are molarized (Deng 2001, 2006; Sun et al. 2018). The Tongxin specimen has straight and smooth nasal bones unlike the genus *Shansirhinus* with a small nasal horn (Deng 2005). According to the typical characteristics of the Tongxin specimen (a small and slender skull; a thin, long, and straight nasal bone; a prominent and rough supraorbital tuberosity; and a short distance between posterior edge of the nasal notch and the orbit), we categorise it in the genus *Aprotodon* (Borissiak 1954; Qiu et al. 2004).

Compared with *A. aralensis* (Borissiak 1954), the Tongxin specimen shares some similarities, such as a flat and long nasal bone with a retracted nasal notch, a short distance between posterior edge of the nasal notch and the orbit, a rhombic and flat frontal surface, and suddenly raised occipital part. However, the Tongxin specimen is smaller in size than *A. aralensis*. The parietal crests of the Tongxin specimen are fused to form a single sagittal crest, whereas the distance between the parietal crests of *A. aralensis* is relatively wider. The end of the nasal bone is slightly upturned in the Tongxin specimen, while that of *A. aralensis* is slightly downturned. The anterior edge of the posterior nares of the Tongxin specimen is V-shaped in outline different from that of *A. aralensis* which is U-shaped in outline. The stoutness of the supraorbital tuberosity of the Tongxin specimen is weaker than that of *A. aralensis*. The differences between the two species in the cheek teeth are also pronounced: the postfossette of *A. aralensis* are larger than that of the Tongxin specimen; the crista on the premolars of *A. aralensis* is weak, but that of the Tongxin specimen is developed and multiple; the lingual cingulum of *A. aralensis* is well developed, whereas that of the Tongxin specimen is reduced, forming a pillar around the entrance of the medisinus.

Different from *A. lanzhouensis* from Lanzhou Basin and Linxia Basin (Qiu and Xie 1997; Qiu et al. 2004), the Tongxin specimen is larger in size. The nasal bones of the Tongxin specimen are thinner than that of *A. lanzhouensis*. The longitudinal height of the nasal notch of the Tongxin specimen is smaller than that of *A. lanzhouensis*. The stoutness of the supraorbital tuberosity of the Tongxin specimen is weaker than that of *A. lanzhouensis*. The anterior margin of the orbit of the Tongxin specimen is retracted at the level of the M2 boundary, but that of *A. lanzhouensis* is located at the level of M1. The anterior edge of the posterior nares of the Tongxin specimen is positioned at the level of M2, while that of *A. lanzhouensis* is located at M3. The cristas on the premolars of the Tongxin specimen are developed and multiple, but those of *A. lanzhouensis* are weak. The crochets on the molars of the Tongxin specimen are stronger than those of *A. lanzhouensis*. The lingual cingulum of the Tongxin specimen is reduced, forming a pillar around the entrance of the medisinus, whereas that of *A. lanzhouensis* is well developed.

The holotype of *A. fatehjangensis* is fragmentary, including P4 and M2. P4 is relatively large, with a strong crochet, paracone fold, and metacone fold different from the P4 of Tongxin specimen with a barely developed weak crochet, weak parastyle fold and paracone rib. Both the protocone and hypocone of the P4 of *A. fatehjangensis* are in regular size with constrictions, while those of the P4 of Tongxin specimen are expanded. The lingual cingulum of the P4 of *A. fatehjangensis* is absent, but that of the P4 of Tongxin specimen is V-shaped at the entrance of the medisinus. M2 of *A. fatehjangensis* has a nearly straight buccal wall, whereas that of Tongxin specimen has a long parastyle and a developed parastyle fold, and a paracone rib with an undulating buccal wall. The lingual cingulum of the M2 of *A. fatehjangensis* is absent, but that of the M2 of Tongxin specimen forms a pillar around the entrance of the medisinus.

A. smith-woodwardi, as the type species of the genus *Aprotodon*, only includes mandibular materials (Forster-Cooper 1915, 1934). Due to the lack of skull material for *A. smith-woodwardi*, we are currently unable to compare the Tongxin specimen with this species.

Therefore, the Tongxin specimen is obviously distinguished from all known species of the genus *Aprotodon* by a unique combination of characters. The skull is slender with thin, long, and straight nasal bones. The nasal notch is high and deep, with the posterior end at the level of the posterior part of P4. The anterior margin of the orbit is positioned at the level of the M2. The distance between the posterior edge of the nasal notch and the orbit is short. The parietal crest forms a sagittal crest. The anterior edge of the posterior nares is V-shaped. The supraorbital tuberosity weaker. The crista is developed and multiple on premolars. The reduced lingual cingulum on molars, forming a pillar around the entrance of the medisinus. Based on these, we refer the Tongxin specimen to a new species, *A. qiui* sp. nov.

Phylogenetic analysis

We conduct a phylogenetic analysis of the Rhinocerotidae to investigate the phylogeny of the Tongxin specimen. The phylogenetic analysis is based on the data matrix of Antoine (2002, 2003) containing 282 morphological characters, with the addition of *Aprotodon qiui* sp. nov., *Aprotodon aralensis*, and *Aprotodon lanzhouensis*. The current matrix consists of 37 taxa coded at the species level. The phylogenetic analysis is performed through a heuristic search using PAUP4.0a169 (Swofford 2002), with TBR. The phylogenetic analysis results in one most parsimonious tree (Figure 3). The tree length is 1225 steps, with a consistency index of 0.2996 and a retention index of 0.5552.

The members of *Aprotodon* are in a stable monophyletic clade. They share twenty-five equivocal synapomorphies including present lateral apophysis of nasal (ch. 1), little developed nuchal tubercle of occipital (ch. 20), dolichocephalic skull (ch. 23), shift antero-externally foramen nervi hypoglossi of basioccipital (ch. 43), fused processus posttympanicus and processus paraoccipitalis (ch. 46), circular foramen magnum of occipital (ch. 49), very upraised symphysis (ch. 53), very massive symphysis (ch. 54), the radio of compared length of the premolars/molars rows between 42% to 50% (ch. 63), always

absent labial cingulum on upper premolars (ch. 83), usually present crochet on P2–4 (ch. 84), wide postfossette on P2–4 (ch. 89), lingual bridge between protocone and hypocone on P2 (ch. 94), always present constriction of the protocone on P3–4 (ch. 101), lingual bridge between protocone and hypocone on P3–4 (ch. 102), always absent antecrochet on P4 (ch. 107), always absent labial cingulum on upper molars (ch. 109), always present crista on upper molars (ch. 112), strong constriction of the protocone on M1–2 (ch. 116), short metaloph on M1–2 (ch. 121), low and reduced posterior cingulum on M1–2 (ch. 124), present posterior groove on the ectometaloph on M3 (ch. 138), external groove developed until the neck on lower cheekteeth (ch. 141), constricted entoconid on lower cheekteeth (ch. 145), always closed postfossette on p2 (ch. 156). All these features support the position of *Aprotodon qiui* as a member of the genus *Aprotodon*, being the sister taxon to *Aprotodon lanzhouensis*.

Conclusion

The almost complete skull from (IVPP V23533) from Tongxin, Ningxia described here is identfied as a teleoceratine of the genus *Aprotodon*, which differs from *Aprotodon aralensis* in its smaller size, with both sides of the parietal crest fused and forming a sagittal crest, the V-shaped anterior edge of the posterior nares, weaker supraorbital tuberosity, and the reduced lingual cingulum on molars, forming a pillar around the entrance of the medisinus; differs from *Aprotodon lanzhouensis* in having thinner nasal bones, posteriorly placed anterior margin of the orbit, strong crochet, developed and multiple crista on premolars, and the reduced lingual cingulum on molars, forming a pillar around the entrance of the medisinus; differs from *Aprotodon fatehjangensis* in smaller size, weak crista on premolars, and the reduced lingual cingulum on molars, forming a pillar around the entrance of the medisinus. Based on these, we herein establish the new species as *A. qiui* sp. nov. Phylogenetic analysis reveals that *A. qiui* sp. nov. and other members of *Aprotodon* are in a stable monophyletic clade. *A. qiui* sp. nov. is the sister taxon to *Aprotodon lanzhouensis*.

Acknowledgments

We thank Wei Gao for his photographs, Xiaocong Guo for her illustrations, Dan Su for her assistance in the repair of the fossil. We are very grateful to the Editor-in -Chief G. Dyke and two anonymous reviewers for their constructive comments and criticisms.

Disclosure statement

No potential conflict of interest was reported by the author(s).

Funding

This research was supported by the National Natural Science Foundation of China (42302013), and the Second Comprehensive Scientific Expedition on the Tibetan Plateau (2019QZKK0705).

References

Antoine P-O. 2002. Phylogénie et Évolution Des Elasmotheriina (Mammalia, Rhinocerotidae). Mémoires du Muséum National d'Histoire Naturelle. 188:1–359.

Antoine PO 2003. Middle miocene elasmotheriine rhinocerotidae from China and Mongolia: taxonomic revision and phylogenetic relationships. Zool Scr. 32:95–118.

Antoine P-O, Downing KF, Crochet J-Y, Duranthon F, Flynn LJ, Marivaux L, Métais G, Rajpar AR, Roohi G. 2010. A revision of *Aceratherium blanfordi* Lydekker, 1884 (Mammalia: Rhinocerotidae) from the Early Miocene of Pakistan: postcranials as a key: Miocene rhinocerotids from Pakistan. Zool J Linn Soc. 160:139–194. doi: 10.1111/j.1096-3642.2009.00597.x.

Beliajeva EI. 1954. New material of Tertiary rhinocerotids. Trans Paleont Inst Acad Sci USSR. 47:24–54.

Borissiak AA. 1954. The oldest *Aceratherium* from Kazakhstan. Trans Paleont Inst Acad Sci USSR. 47:5–23.

Cerdeño E. 1995. Cladistic analysis of the family Rhinocerotidae (Perissodactyla). Am Mus Novit. 3143:1–25.

Deng T. 2000. A new species of *Acerorhinus* (Perissodactyla, Rhinocerotidae) from the Late Miocene in Fugu, Shaaxi, China. Vert PalAs. 38:203–217.

Deng T. 2001. New materials of *Chilotherium wimani* (Perrisodactyla, Rhinocerotidae) from the Late Miocene of Fugu, Shaanxi. Vert PalAs. 39:129–138.

Deng T. 2004. A new species of the rhinoceros *Alicornops* from the middle Miocene of the Linxia Basin, Gansu, China. Palaeontology. 47:1427–1439. doi: 10.1111/j.0031-0239.2004.00420.x.

Deng T. 2005. New cranial material of *Shansirhinus* (Rhinocerotidae, Perissodactyla) from the lower pliocene of the Linxia Basin in Gansu, China. Geobios. 38:301–313. doi: 10.1016/j.geobios.2003.12.003.

Deng T 2006. A primitive species of chilotherium (perissodactyla, rhinocerotidae) from the late miocene of the Linxia Basin. (Gansu, China). Cainozoic Research. 5:93–102.

Deng T. 2013. Incisor fossils of *Aprotodon* (Perissodactyla, Rhinocerotidae) from the Early Miocene shangzhuang Formation of the Linxia Basin in Gansu, China. Vert PalAs. 51:131–140.

Forster-Cooper C. 1915. XLIX.—new genera and species of mammals from the Miocene deposits of Baluchistan.—preliminary notice. The Annals And Magaz of Nat His. 16(95):404–410. doi: 10.1080/00222931508693732

Forster-Cooper C. 1934. XIII. The extinct of rhinoceroses of Baluchistan. *Philosophical Transactions of the Royal Society of London*. Series B, Containing Papers Biological Char. 223:569–616. doi: 10.1098/rstb.1934.0013.

Geraads D, Miller E. 2013. *Brachypotherium minor* n. sp., and other Rhinocerotidae from the Early Miocene of Buluk, Northern Kenya. Geodiversitas. 35:359–375. doi: 10.5252/g2013n2a5.

Guérin C. 1980. Les rhinocéros (Mammalia, Perissodactyla) du Miocène terminal au Pléistocène supérieur en Europe occidentale. Comparaison avec les espèces actuelles (fascicule 1). Travaux et Documents des Laboratoires de Géologie de Lyon. 79:1–1184.

Heissig K. 1972. Paläontologische und geologische Untersuchungen im Tertiär von Pakistan. 5. Rhinocerotidae (mamm.) aus den unteren und mittleren Siwalik-Schichten. Abhandlungen der Bayerischen Akademie der Wissenschaften. 152:1–112.

Heissig K. 1989. The Rhinocerotidae. In "the evolution of Perissodactyls" (DR Prothero and RM schoch, eds.). New York: Oxford Univ. Press.

Heissig K. 1999. Family Rhinocerotidae. In: Rössner G. E. Heissig K, editors. The miocene land mammals of Europe. Munich: Verlag Dr. F. Pfeil; pp. 175–188.

Li Z, Li Y, Zhang Y, Xie K, Zhichao L, Chen Y. 2021. New material of *Aprotodon lanzhouensis* (Perissodactyla, Rhinocerotidae) from the Early Miocene in Northwest China. Geological J. 56(9):4779–4787. doi: 10.1002/gj.4212

Pilgrim GE. 1912. The vertebrate fauna of the Gaj series in the Bugti Hills and Punjab. Paleontologia Indica. 4:1–83.

Qiu ZX, Wang BY, Deng T. 2004. Mammal fossils from Yagou, Linxia Basin, Gansu, and related stratigraphic problems. Vert PalAsiat. 42:276–296.

Qiu Z, Xie J. 1997. A new species of *Aprotodon* (Perissodactyla, Rhinocerotidae) from Lanzhou Basin, Gansu, China. Vert PalAs. 35:250–267.

Qiu ZX, Xie JY, Yan DF. 1988. A new chilothere skull from Hezheng, Gansu, China, with special reference to the Chinese "*Diceratherium*". Sci SinSer B. 31:494–502.

Sun D, Li Y, Deng T. 2018. A new species of *Chilotherium* (Perissodactyla, Rhinocerotidae) from the Late Miocene of Qingyang, Gansu, China. Vert PalAs. 56:216–228.

Swofford DL. 2002. PAUP*. Phylogenetic analysis using parsimony (*and other methods) version 4. Sunderland, Massachusetts: Sinauer Associates.

Wang BY, Qiu ZX, Zhang QZ, Wu LJ, Ning PJ. 2009. Large mammals found from Houldjin Formation near Erenhot, Nei Mongol, China. Vert PalAs. 47:85–110.

Yan DF. 1983. Über die klassifikation und morphologie des schädel von *Plesiaceratherium*. Vert PalAs. 21:134–143.